# Search for Supersymmetry with Gauge-Mediated Breaking in Diphoton Events with Missing Transverse Energy at CDF II

(Dated: August 25, 2009; Version 2.0)

We present the results of a search for supersymmetry with gauge-mediated breaking and $\widetilde{\chi}_1^0 \to \gamma\widetilde{G}$ in the $\gamma\gamma$+missing transverse energy final state. In 2.6±0.2 fb$^{-1}$ of $p\bar{p}$ collisions at $\sqrt{s}$=1.96 TeV recorded by the CDF II detector we observe no candidate events, consistent with a standard model background expectation of 1.4±0.4 events. We set limits on the cross section at the 95% C.L. and place the world's best limit of 149 GeV/c$^2$ on the $\widetilde{\chi}_1^0$ mass at $\tau_{\widetilde{\chi}_1^0}$=0 ns. We also make exclusions in the $\widetilde{\chi}_1^0$ mass-lifetime plane for $\tau_{\widetilde{\chi}_1^0} \lesssim$2 ns.

PACS numbers: 13.85.Rm, 12.60.Jv, 13.85.Qk, 14.80.Ly

The standard model (SM) of elementary particles has been enormously successful, but is incomplete. Theoretical motivations [1] and the observation of the '$ee\gamma\gamma$+missing transverse energy ($\not\!\!E_{\rm T}$)' [2, 3] candidate event by the CDF experiment during Run I at the Fermilab Tevatron provide compelling rationale to search for the production and decay of new heavy particles that produce events with final state photons and $\not\!\!E_{\rm T}$ in collider experiments. Of particular theoretical interest are supersymmetry (SUSY) models with gauge-mediated SUSY-breaking (GMSB) [1]. These models solve the "naturalness problem" [4] and provide a low-mass dark matter candidate that is both consistent with inflation and astronomical observations [5]. Since many versions of these models have a similar phenomenology, we consider a scenario in which the lightest neutralino ($\tilde{\chi}_1^0$) decays almost exclusively (>96%) into a photon ($\gamma$) and a weakly interacting, stable gravitino ($\tilde{G}$) that gives rise to $\not\!\!E_{\rm T}$ by leaving the detector without depositing any energy [6]. In these models, the $\widetilde{\chi}_1^0$ is favored to have a lifetime on the order of a nanosecond, and the $\tilde{G}$ is a warm dark matter candidate with a mass in the range $0.5<m_{\tilde{G}}<1.5$ keV/$c^2$ [7]. Other direct searches [8–10] have constrained the mass of the $\tilde{\chi}_1^0$ to be greater than 100 GeV/c$^2$ for much of the parameter space. At the Tevatron sparticle production is predicted to be primarily into gaugino pairs, and the $\widetilde{\chi}_1^0$ mass ($m_{\widetilde{\chi}_1^0}$) and lifetime ($\tau_{\widetilde{\chi}_1^0}$) are the two most important parameters in determining the final states and their kinematics. Different search strategies are required for $\widetilde{\chi}_1^0$ lifetimes above and below about a nanosecond [11].

In this Letter we describe a search for GMSB, in which gaugino pairs are produced and decay to the $\gamma\gamma+\not\!\!E_{\rm T}+X$ final state where $X$ denote other high-$E_{\rm T}$ final state particle [12]. We use a dataset corresponding to an integrated luminosity of 2.6±0.2 fb$^{-1}$ of $p\bar{p}$ collisions at $\sqrt{s}$=1.96 TeV from the Tevatron collected with the CDF II detector [13]. This dataset is ten times larger than the one used in our previous search [8]. For the first time in this channel we use a new photon timing system [14] and a new model of the $\not\!\!E_{\rm T}$ resolution (METMODEL) [15]. These additions significantly enhance our rejection of backgrounds from instrumental and non-collision sources, which allows us to considerably extend the sensitivity of the search for large $\widetilde{\chi}_1^0$ masses compared to other Tevatron searches [9]. We also extend the search to consider $\widetilde{\chi}_1^0$ lifetimes up to 2 ns which are favored for larger $m_{\tilde{\chi}_1^0}$.

Our strategy is to select $\gamma\gamma$ candidates and optimize the search for the presence of both significant $\not\!\!E_{\rm T}$ and large total event transverse energy to indicate the decays of heavy gauginos. We perform an *a priori* analysis based on the expected sensitivity, taking into account backgrounds from SM with mismeasured ("fake") $\not\!\!E_{\rm T}$, electroweak production with real $\not\!\!E_{\rm T}$, and non-collision sources and signal predictions.

Here we briefly describe the aspects of the detector [13] relevant to this analysis. The magnetic spectrometer consists of tracking devices inside a 3-m diameter, 5-m long superconducting solenoid magnet that operates at 1.4 T. A 3.1-m long drift chamber (COT) with 96 layers of sense wires measures the $z$ position, time of the $p\bar{p}$ interaction, and the momenta of charged particles. The calorimeter consists of projective towers with electromagnetic (EM) and hadronic (HAD) compartments and is divided into a central barrel that surrounds the solenoid coil ($|\eta|<1.1$) [2] and a pair of end-plugs that cover the region $1.1<|\eta|<3.6$. Both are used to identify and measure the 4-momenta of photons, electrons, and jets ($j$) [16] and provide $\not\!\!E_{\rm T}$ information. The EM calorimeter is instrumented with a timing system, EMTiming [14], that measures the arrival time of photons.

Our analysis begins with events passing the CDF three-level trigger. The combined trigger selection efficiency is effectively 100% for our diphoton events with two photons with $|\eta|<1.1$ and $E_{\rm T}>13$ GeV [15]. Offline, both photons are required to be in the fiducial part of the calorimeter and to pass the standard CDF photon identification (ID) and isolation requirements [8] with two minor modifications to remove instrumental and electron backgrounds [15, 17]. The remaining events are dominated by SM production of $\gamma\gamma$, $\gamma j$ with $j\to\gamma_{fake}$, and $jj\to\gamma_{fake}\gamma_{fake}$, where $\gamma_{fake}$ is a jet misidentified as a photon. To minimize the number of these events with large $\not\!\!E_{\rm T}$ due to calorimeter energy mismeasurements we remove events if the $\not\!\!E_{\rm T}$ vector points within

$|\Delta\phi|<0.3$ of the second highest $E_{\rm T}$ photon or any jet pointing to an uninstrumented region of the calorimeter [15]. We require the primary collision vertex position with $|z_{\rm vertex}|<60$ cm to reduce non-collision backgrounds and maintain the projective nature of the photon reconstruction in the calorimeter. For events with multiple reconstructed vertices we change the photon $E_{\rm T}$ and $\not\!\!E_{\rm T}$ values if picking a different vertex for them reduces the event $\not\!\!E_{\rm T}$.

Non-collision backgrounds coming from cosmic rays and beam-related effects can produce $\gamma\gamma$+$\not\!\!E_{\rm T}$ candidates, and are removed from the inclusive $\gamma\gamma$ sample using a number of techniques. Photon candidates from cosmic rays are not correlated in time with collisions and events are removed if the timing of either photon, corrected for average path length ($t_\gamma$), indicates a non-collision source [15, 17]. Photon candidates can also be produced by beam-related muons that originate upstream of the detector. These are suppressed using standard beam halo identification requirements [17]. A total of 38,053 inclusive $\gamma\gamma$ candidate events pass all the selection requirements.

Backgrounds to the $\gamma\gamma$+$\not\!\!E_{\rm T}$ final state from SM $\gamma\gamma$/ $\gamma\gamma_{fake}$/$\gamma_{fake}\gamma_{fake}$ and fake $\not\!\!E_{\rm T}$ arise due to energy mismeasurements in the calorimeter or event reconstruction pathologies. We use the METMODEL to select events with real and significant $\not\!\!E_{\rm T}$, as part of the optimization, and to predict the contribution of SM backgrounds with fake $\not\!\!E_{\rm T}$ due to normal energy measurement fluctuations. This algorithm considers the clustered (jets) and unclustered energy in the event and calculates a probability for fluctuations in the energy measurement to produce $\not\!\!E_T{}^{fluct}$ equivalent to or larger than the measured $\not\!\!E_{\rm T}$ ($P_{\not\!\!E_T{}^{fluct}\geq\not\!\!E_{\rm T}}$). This probability is then used to define a $\not\!\!E_{\rm T}$-significance as $-\log_{10}\left(P_{\not\!\!E_T{}^{fluct}\geq\not\!\!E_{\rm T}}\right)$. Events with true and fake $\not\!\!E_{\rm T}$ of the same value have, on average, different $\not\!\!E_{\rm T}$-significance. We use pseudo-experiments to estimate the expected $\not\!\!E_{\rm T}$-significance distribution for SM events with fake $\not\!\!E_{\rm T}$, and the number of mismeasured events above a given $\not\!\!E_{\rm T}$-significance requirement. The jets and unclustered energy are smeared according to their resolution functions in the event. The systematic uncertainty in the METMODEL is dominated by the uncertainty in the resolution functions [15].

The METMODEL does not account for reconstruction pathologies in SM events with no intrinsic $\not\!\!E_{\rm T}$, such as a wrong choice of the primary interaction vertex or triphoton events with a lost photon. To obtain the prediction for this background we model SM kinematics and event reconstruction using a PYTHIA Monte Carlo (MC) [18] $\gamma\gamma$ sample with a detector simulation [19]. Since this sample does not include contributions from $\gamma j$ and $jj$ sources, but pathologies are likely to be the same, we normalize to the number of events in the inclusive $\gamma\gamma$ data sample. We subtract the expectations for energy mismeasurement fluctuations in the MC to avoid double counting. Uncertainties are dominated by the statistics of the MC sample.

Electroweak production of $W$ and $Z$ bosons which decay to leptons can also give rise to the $\gamma\gamma$+$\not\!\!E_{\rm T}$ signature where one or more of the photons can be fake, but the $\not\!\!E_{\rm T}$ is due to one or more neutrinos. To estimate the contribution from these backgrounds we use MC simulations, normalized to their theoretical cross sections and taking into account all the leptonic decay modes. The Baur MC [20] is used to simulate $W\gamma$ and $Z\gamma$ production and decay where initial and final state radiation (ISR/FSR) produce $W/Z$+$\gamma\gamma$ events. The PYTHIA MC is used to simulate backgrounds where both photons are fakes: $W$, $Z$, with photons from ISR/FSR removed, and $t\bar{t}$ sources. To minimize the dependence of our predictions on potential "MC-data" differences we scale our MC predictions to the observed number of $e\gamma$ events [15] in data where we use the same diphoton triggers and analysis selection procedures used to select the inclusive $\gamma\gamma$ sample. Uncertainties are dominated by the statistics of the MC and $e\gamma$ normalization data sample.

Non-collision backgrounds are estimated using the data. Using the inclusive $\gamma\gamma$ sample selection requirements, but requiring one of the photons to have $t_\gamma>25$ ns we identify a cosmic-enhanced sample. Similarly, we select a beam-related background enhanced sample. We estimate the number of these events in the signal region using the ratio of events outside the timing requirements to events inside the signal region and the measured efficiencies of the non-collision rejection requirements [15]. The uncertainties on both non-collision background estimates are dominated by the statistical uncertainty on the number of identified events. The top of Figure 1 shows the $\not\!\!E_{\rm T}$-significance distribution for the inclusive $\gamma\gamma$ sample, along with the predictions for all the backgrounds.

We estimate the sensitivity to heavy, neutral particles that decay to photons using the GMSB reference model [6] in the mass-lifetime range, $75\leq m_{\tilde{\chi}_1^0}\leq 150$ GeV and $\tau_{\tilde{\chi}_1^0}\lesssim 2$ ns. Events from all SUSY processes [21] are simulated with PYTHIA followed by a detector simulation. The fraction of $\tilde{\chi}_1^0$ decays that occur in the detector volume, and thus the acceptance, are dependent on both the lifetime and the masses of the sparticles [11]. The total systematic uncertainty on the acceptance, after all kinematic requirements, is estimated to be 7%, dominated by the uncertainty in the photon ID efficiency (2.5% per photon). Other significant contributions come from uncertainties on ISR/FSR (4%), jet energy measurement (2%), $\not\!\!E_{\rm T}$-significance parameterizations (1%) and the parton distribution functions (1%).

We determine the final kinematic selection requirements by optimizing the mean expected 95% confidence level (C.L.) cross section limit using a no-signal assumption, before looking at the data in the signal region [22]. To compute the predicted cross section upper limit we

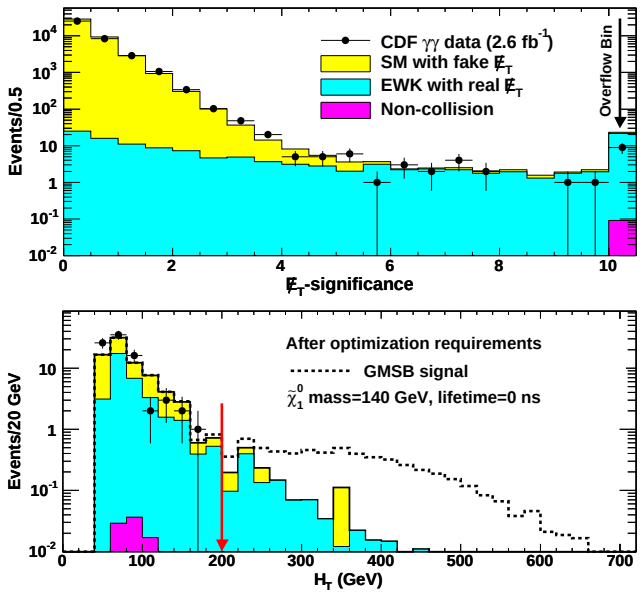


FIG. 1: The top plot shows the $\not\!\!E_{\rm T}$-significance distribution for the inclusive $\gamma\gamma$ candidate sample, along with the background predictions. The bottom plot shows the predicted $H_{\rm T}$ (total $E_{\rm T}$ of photons, jets, and $\not\!\!E_{\rm T}$) distribution after all but the final $H_{\rm T}$ requirement.

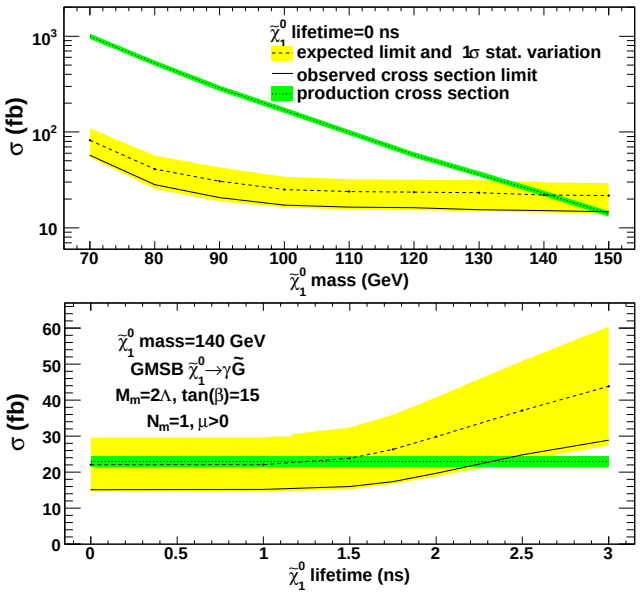


FIG. 2: The predicted and observed 95% C.L. cross section upper limits as a function of the $\widetilde{\chi}_1^0$ mass at a lifetime of 0 ns (top) and as a function of the $\widetilde{\chi}_1^0$ lifetime at a mass of 140 GeV/$c^2$ (bottom). Indicated in green (darker shading) is the production cross section, along with its 8.0% uncertainty-band. In yellow (lighter shading) is the RMS variation on the expected cross section limit.

combine the luminosity, the acceptance and the background estimates with their systematic uncertainties using a Bayesian method [23]. The predicted limits are optimized by simultaneously varying the selection requirements for $\not\!\!E_{\rm T}$-significance, $H_{\rm T}$ (scalar sum of $E_{\rm T}$ of photons, jets, and $\not\!\!E_{\rm T}$), and the azimuthal angle between the two leading photons, $\Delta\phi(\gamma_1,\gamma_2)$. The large $\not\!\!E_{\rm T}$-significance requirement eliminates most of the SM background with fake $\not\!\!E_{\rm T}$. GMSB production is dominated by heavy gaugino pairs which decay to high-$E_{\rm T}$ light final state particles via cascade decays. The GMSB signal has, on average, larger $H_{\rm T}$ compared to SM backgrounds so that an $H_{\rm T}$ requirement can remove these backgrounds effectively. Electroweak backgrounds with large $H_{\rm T}$ typically consist of a high-$E_{\rm T}$ photon recoiling against $W\to e\nu$, identified as $\gamma_{fake}\not\!\!E_{\rm T}$, which means the gauge boson decay is highly boosted. Thus, the two photon candidates in the final state are mostly back-to-back. Also, the high-$E_{\rm T}$ diphotons with large $H_T$ from SM background are mostly back-to-back with fake $\not\!\!E_{\rm T}$; the $\Delta\phi(\gamma_1,\gamma_2)$ cut, therefore, reduces both these backgrounds.

Each point in the considered $\tau_{\tilde{\chi}_1^0}$ vs. $m_{\tilde{\chi}_1^0}$ space gives a slightly different optimization. We choose a single set of requirements to maximize the region where the predicted production cross section at next-to-leading order [24] is above the expected 95% C.L. cross section limit. The exclusion region also takes into account the production cross section uncertainties, which are dominated by the parton distribution functions (7%) and the renormalization scale (3%). We find the optimal set of cuts, before unblinding the signal region, to be: $\not\!\!E_{\rm T}$-significance>3, $H_{\rm T}$>200 GeV, and $\Delta\phi(\gamma_1,\gamma_2)<\pi-0.35$. With these requirements we predict 1.4±0.4 background events, 0.9±0.4 of which is from electroweak sources (dominated by $Z\gamma$ production) with real $\not\!\!E_{\rm T}$, 0.5±0.2 from SM with fake $\not\!\!E_{\rm T}$, and $0.001^{+0.008}_{-0.001}$ from non-collision sources. The acceptance for $m_{\tilde{\chi}_1^0}$=140 GeV/c$^2$ and $\tau_{\tilde{\chi}_1^0}$=0 ns is estimated to be 7.8±0.6%.

No events in the data pass the final event selection. The predicted $H_{\rm T}$ distribution is shown in Figure 1 (bottom), after all but the final $H_{\rm T}$ cut. The data is consistent with the no-signal hypothesis and well modeled by backgrounds alone. We set cross section limits as a function of $m_{\tilde{\chi}_1^0}$ and $\tau_{\tilde{\chi}_1^0}$ respectively, as shown in Figure 2. The $m_{\tilde{\chi}_1^0}$ reach, based on the predicted and observed number of events for $\tau_{\tilde{\chi}_1^0}$=0, is 141 GeV/c$^2$ and 149 GeV/c$^2$ respectively. These limits significantly extend the search sensitivity beyond the results of D0 [9], expand the results to include exclusions for $\tau_{\tilde{\chi}_1^0}\leq$2 ns, and, when combined with the complementary limits from CDF and LEP [10, 17], cover the region shown in Figure 3.

In conclusion, we have performed an optimized search for heavy, neutral particles that decay to photons in the $\gamma\gamma$+$\not\!\!E_{\rm T}$ final state using 2.6±0.2 fb$^{-1}$ of data. There is no excess of events beyond expectations. We set cross section limits using a GMSB model with $\widetilde{\chi}_1^0\to\gamma\widetilde{G}$, and

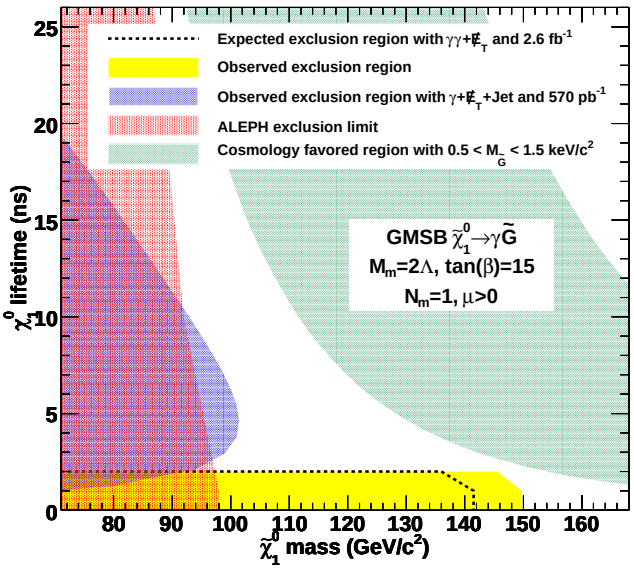


FIG. 3: The predicted and observed exclusion region along with the limit from ALEPH/LEP [10] and the CDF $\gamma$+$\not\!\!E_{\rm T}$+*jet* 'delayed' photon analysis [17]. We have a mass reach of 141 GeV/$c^2$ (predicted) and 149 GeV/$c^2$ (observed) at lifetimes up to 1 ns. The shaded band shows the parameter space where $0.5<m_{\tilde{G}}<1.5$ keV/$c^2$, favored by cosmological models [7].

find an exclusion region in the $\tau_{\tilde{\chi}_1^0}$-$m_{\tilde{\chi}_1^0}$ plane with the world's best 95% C.L. lower limit on the $\widetilde{\chi}_1^0$ mass of 149 GeV/c$^2$ at $\tau_{\tilde{\chi}_1^0}$=0 ns. By the end of Run II, with an integrated luminosity of 10 fb$^{-1}$, we estimate a mass reach of $\simeq$ 160 GeV/c$^2$ at a lifetime of 0 ns.

We thank the Fermilab staff and the technical staffs of the participating institutions for their vital contributions. This work was supported by the U.S. Department of Energy and National Science Foundation; the Italian Istituto Nazionale di Fisica Nucleare; the Ministry of Education, Culture, Sports, Science and Technology of Japan; the Natural Sciences and Engineering Research Council of Canada; the National Science Council of the Republic of China; the Swiss National Science Foundation; the A.P. Sloan Foundation; the Bundesministerium für Bildung und Forschung, Germany; the Korean Science and Engineering Foundation and the Korean Research Foundation; the Particle Physics and Astronomy Research Council and the Royal Society, UK; the Russian Foundation for Basic Research; the Comisión Interministerial de Ciencia y Tecnología, Spain; in part by the European Community's Human Potential Programme under contract HPRN-CT-2002-00292; and the Academy of Finland.

[1] S. Dimopoulos, S. Thomas, and J. Wells, Nucl. Phys. B **488**, 39 (1997); S. Ambrosanio, G. Kribs, and S. Martin, Phys. Rev. D **56**, 1761 (1997); G. Giudice and R. Rattazzi, Phys. Rep. **322**, 419 (1999); S. Ambrosanio, G. Kane, G. Kribs, S. Martin, and S. Mrenna, Phys. Rev. D **55**, 1372 (1997).

[2] We use a cylindrical coordinate system in which the proton beam travels along the $z$-axis, $\theta$ is the polar angle, $\phi$ is the azimuthal angle relative to the horizontal plane, and $\eta$=$-\ln\tan(\theta/2)$. The transverse energy and momentum are defined as $E_T$=$E\sin\theta$ and $p_T$=$p\sin\theta$ where $E$ is the energy measured by the calorimeter and $p$ the momentum measured in the tracking system. $\not\!\!E_{\rm T}$=$|-\sum_i E_T^i\vec{n}_i|$ where $\vec{n}_i$ is a unit vector that points from the interaction vertex to the $i^{\rm th}$ calorimeter tower in the transverse plane.

[3] F. Abe *et al.* (CDF Collaboration), Phys. Rev. Lett. **81**, 1791 (1998) and Phys. Rev. D **59**, 092002 (1999).

[4] S. Martin, arXiv:hep-ph/9709356.

[5] P. Bode, J. Ostriker, and N. Turok, Astrophys. J. **556**, 93 (2001).

[6] B. Allanach *et al.*, Eur. Phys. J. C**25**, 113 (2002). We use benchmark model 8 and take the messenger mass scale $M_{\rm mess}$=2Λ, tan($\beta$)=15, $\mu$>0 and the number of messenger fields $N_{\rm mess}$=1. The $\tilde{G}$ mass factor and the supersymmetry breaking scale Λ are allowed to vary independently.

[7] C.-H. Chen and J. Gunion, Phys. Rev. D **58**, 075005 (1998).

[8] D. Acosta *et al.* (CDF Collaboration), Phys. Rev. D **71**, 031104 (2005).

[9] V. Abazov *et. al.* (D0 Collaboration), Phys. Lett. B **659**, 856 (2008).

[10] A. Heister *et al.* (ALEPH Collaboration), Eur. Phys. J. C **25**, 339 (2002); also see M. Gataullin, S. Rosier, L. Xia and H. Yang, arXiv:hep-ex/0611010; G. Abbiendi *et al.* (OPAL Collaboration), Proc. Sci. HEP2005 346 (2006); J. Abdallah *et al.* (DELPHI Collaboration), Eur. Phys. J. C **38** 395 (2005).

[11] D. Toback and P. Wagner, Phys. Rev. D **70**, 114032 (2004).

[12] E. Lee, Ph.D. thesis, Texas A&M University, 2009.

[13] D. Acosta *et al.* (CDF Collaboration), Phys. Rev. D **71**, 032001 (2005).

[14] M. Goncharov *et al.*, Nucl. Instrum. Methods A**565**, 543 (2006).

[15] T. Aaltonen *et al.* (CDF Collaboration), *Search for Anomalous Prodcution of Events with Two Photons and Additional Energetic Objects at CDF*, to be submitted to Phys. Rev. D. Photons with second highest $E_{\rm T}$ or narrow jets that occur in few towers and have few tracks, can be mismeasured if they are located close to the calorimeter cracks at $\eta\sim 0$ and $|\eta|\sim 1.1$.

[16] For a discussion of the jet energy measurements, see T. Affolder *et al.*(CDF Collaboration), Phys. Rev. D. **64**, 032001 (2001). For a discussion of standard jet correction systematics, see A. Bhatti *et al.*, Nucl. Instrum. Methods, A 566, 375 (2006). We use jets with cone size $\Delta R$=0.4.

[17] A. Abulencia *et al.* (CDF Collaboration), Phys. Rev. Lett. **99**, 121801 (2007); T. Aaltonen *et al.* (CDF Collaboration), Phys. Rev. D **78**, 032015 (2008).

[18] T. Sjöstrand *et al.*, Comput. Phys. Commun. **135**, 238 (2001). We use version 6.216.
[19] We use the standard GEANT based detector simulation [R. Brun *et al.*, CERN-DD/EE/84-1 (1987)] and add a parametrized EMTiming simulation.
[20] U. Baur, T. Han and J. Ohnemus, Phys. Rev. D **48**, 5140 (1993); U. Baur, T. Han and J. Ohnemus, *ibid.* **57**, 2823 (1998); The $W\gamma$ and $Z\gamma$ processes are simulated using the leading-order event generator and have a k-factor fixed at 1.36. Initial and final state radiation (resulting in additional jets or photons), underlying event, and additional interactions are simulated using PYTHIA [18].
[21] P. Simeon and D. Toback, J. Undergrad. Research in Phys. 20, 1 (2007).
[22] E. Boos, A. Vologdin, D. Toback, and J. Gaspard, Phys. Rev. D **66**, 013011 (2002).
[23] T. Junk, Nucl. Instrum. Methods A**434**, 435-443 (1999).
[24] We use the leading-order cross sections generated by PYTHIA [18] and the k-factors produced by PROSPINO 2.0 [W. Beenakker *et al.*, Phys. Rev. Lett. **83**, 3780 (1999)].